Archives of Materials Science and Engineering

Volume 105
Issue 1
September 2020
Pages 17-30

International Scientific Journal
published monthly by the
World Academy of Materials
and Manufacturing Engineering

DOI: 10.5604/01.3001.0014.5120

Estimation of discharge correction factor of modified Parshall flume using ANFIS and ANN

D. Saran *, N.K. Tiwari
Department of Civil Engineering, National Institute of Technology Kurukshetra, India
* Corresponding e-mail address: diwakarsaran31@gmail.com
ORCID identifier: https://orcid.org/0000-0002-3153-2531 (N.K.T.)

ABSTRACT

Purpose: To evaluate and compare the capability of ANFIS (Adaptive Neuro-Fuzzy-Inference System), ANN (Artificial Neural Network), and MNLR (Multiple Non-linear Regression) techniques in the estimation and formulation of Discharge Correction Factor (C_d) of modified Parshall flumes as based on linear relations and errors between input and output data.

Design/methodology/approach: Acknowledging the necessity of further research in this field, experiments were conducted in the Hydraulics Laboratory of Civil Engineering Department, National Institute of Technology, Kurukshetra, India. The Parshall flume characteristics, associated longitudinal slopes and the discharge passing through the flume were varied. Consequent water depths at specific points in Parshall flumes were noted and the values of C_d were computed. In this manner, a data set of 128 observations was acquired. This was bifurcated arbitrarily into a training dataset consisting of 88 observations and a testing dataset consisting of 40 observations. Models developed using the training dataset were checked on the testing dataset for comparison of the performance of each predictive model. Further, an empirical relationship was formulated establishing C_d as a function of flume characteristics, longitudinal slope, and water depth at specific points using the MNLR technique. Moreover, C_d was estimated using soft computing tools; ANFIS and ANN. Finally, a sensitivity analysis was done to find out the flume variable having the greatest influence on the estimation of C_d.

Findings: The predictive accuracy of the ANN-based model was found to be better than the model developed using ANFIS, followed by the model developed using the MNLR technique. Further, sensitivity analysis results indicated that primary depth reading (H_a) as input parameter has the greatest influence on the prediction capability of the developed model.

Research limitations/implications: Since the soft computing models are data based learning, hence the prediction capability of these models may dwindle if data is selected beyond the current data range, which is based on the experiments conducted under specific conditions. Further, since the present study has faced time and facility constraints, hence there is still a huge scope of research in this field. Different lateral slopes, combined lateral-longitudinal slopes, and more modified Parshall flume models of larger sizes can be added to increase the versatility of the current research.

Practical implications: C_d of modified Parshall flumes can be predicted using the ANN-based prediction model more accurately as compared to other considered techniques.

Originality/value: The comparative analysis of prediction models, as well as the formulation of relation, has been conducted in this study. In all the previous works, little to no soft computing techniques have been applied for the analysis of Parshall flumes. Even the regression techniques have been applied only on Parshall flumes of standard sizes. However, this paper includes not only Parshall flume of standard size but also a modified Parshall flume in its pursuit of predicting C_d with the help of ANN and ANFIS based prediction models along with MNLR technique.

Keywords: Parshall flumes, Discharge Correction Factor, Adaptive Neuro-Fuzzy Inference System, Artificial Neural Network, Multiple Non-linear Regression

Reference to this paper should be given in the following way:

D. Saran, N.K. Tiwari, Estimation of discharge correction factor of modified Parshall flume using ANFIS and ANN, Archives of Materials Science and Engineering 105/1 (2020) 17-30. DOI: https://doi.org/10.5604/01.3001.0014.5120

METHODOLOGY OF RESEARCH, ANALYSIS AND MODELLING

1. Introduction

It becomes a matter of prime importance for a hydraulic engineer to accurately measure the irrigation water as it is conveyed to the farmers from canals and ditches [1]. Defective measurements lead to a reduction in the supply of water to farms to such an extent that it causes a serious hindrance in the full maturity of crops, thus causing insurmountable losses to the farmer [2].

Weirs were one of the earliest devices which were installed for accurate measurement of discharge. However, high loss of head, combined with constant choking of weirs due to debris, demanded periodic maintenance of weirs. As a result, over the years, the popularity of weirs decreased [3].

These problems ended with the invention of Parshall Flume, created by R.L. Parshall in 1928. Originally known as "Improved Venturi Flume", it was a modified version of Venturi Flume created by V.M. Cone in 1917. The basic modifications were the reduction in convergence and divergence angles, along with the elongation of throat and inclusion of a drop through the throat of the flume [1,4]. Due to the presence of converging side walls as well as drop in the floor, the water passing through the flume is accelerated and gradually transforms from subcritical flow to supercritical flow. As a result, the problem of choking of flume due to debris is eliminated [5]. Furthermore, accurate measurement of discharge now becomes possible by taking just one water depth reading at a specific point in the flume [1,2,6,7]. The sketch of the Parshall Flume has been shown in Figure 1.

Hordes of studies have been conducted by various investigators around the world, providing different formulae for the calculation of discharge. S.R. Abt, et.al. [8] conducted experiments on a 7.62 cm Parshall flume at varying longitudinal slopes and provided a formula for measurement of discharge. Similarly, S.R. Abt, et.al. [9]

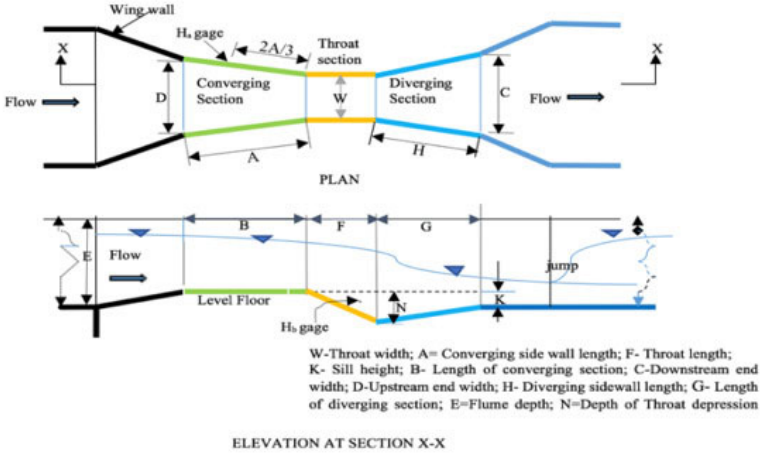

Fig. 1. Sketch of Parshall flume

ran experiments on the Parshall flume of the same size, however in this case the discharge measurement formula was established taking into account the effect of lateral slopes. This was followed by A. Genovez, et.al. [10], who carried out experiments on 30.5 cm and 61 cm flumes. Here the effects of all three i.e., lateral slopes, longitudinal slopes, and combined lateral-longitudinal slopes were studied, with correction factors being formulated for each of the three effects. The results of the study were then compared with the similarly conducted tests on 2.54 cm, 5.08 cm, and 7.62 cm Parshall Flumes. Subsequently, S. Abt, et.al. [11] conducted experiments on 30.5 cm Parshall flume under different lateral slopes. In this case, variation in submergence conditions was also introduced. Henceforth, 2 corrections, one for submerged conditions and another for lateral slopes were formulated in this case. Similar, but advanced experiments were performed by S.R. Abt, et.al. [12] on 2.54 cm, 5.08 cm, 7.62 cm, 30.4 cm, and 61 cm size flumes under varying lateral slopes, longitudinal slopes, and submergence conditions, with correction factors being formulated for each anomaly. B.J. Heiner, et.al. [13] carried out experiments on 61 cm Parshall flume and studied the effects of incorrect Staff Gauge location as well as absence and incorrect design of entrance wing walls on the discharge formula of the flume. Accordingly, correction factors were given for each anomaly.

The application of Soft computing and regression techniques has notably gained popularity in recent times. New artificial intelligence methods have been successfully applied for the prediction of required data. Correction factors have been computed successfully using linear regression analysis and multiple variable regression analysis by [8-12]. Further, prediction models have been developed in recent times using soft computing techniques during the analysis of various aspects of Parshall flumes. B.M. Savage, et.al. [14] used Flow 3D, a Computational fluid dynamics (CFD) software to validate the usage of numerical modelling in creating discharge correction coefficients for Parshall Flumes of different sizes possessing varying head location conditions and entrance locations. N.K. Tiwari, et.al. [15] used ANFIS, ANN, and Fuzzy Logic for the prediction of oxygen transfer in the case of modified Parshall flumes. Similarly, M. Kumar, et.al. [16] applied Kernel function based regression approaches for estimating the oxygen transfer performance of plunging hollow jet aerator. Finally, D. Bodana, et.al. [17] applied ANN as well as Gaussian process regression (GPR) for the estimation of penetration depth in plunging hollow jet.

In this work, the predictive accuracy of Adaptive neuro-fuzzy inference system (ANFIS), Artificial neural network (ANN), and Multiple nonlinear regression (MNLR) techniques have been analyzed by checking the prediction of C_d by the above-mentioned techniques. This was done using the data obtained by conducting various experiments in the laboratory. The value of C_d has been correlated with six variables: Throat width (W), Throat length (F), Sill height (K), Longitudinal slope (S), water depth reading at primary point (H_a), and at a secondary point (H_b) in the flume. The performance of the developed models was compared amongst themselves. Finally, sensitivity analysis was carried out to find the most influential input parameter.

2. Materials and methods

2.1. Experimental setup and collection of data

The experiments were conducted in a standard recirculating channel 4 m long, 0.25 m wide, and 0.30 m deep. The channel possessed a maximum discharge capacity of approximately 6 L/s. It was connected to a recirculating closed device, which continuously supplied water to the channel by redrawing water from the storage tank 1.27 m long, 0.635 m wide, and 0.635 m deep. The actual discharge through the channel was measured with the help of Cipoletti Weir installed downstream of the channel, using the formula [18];

$$Q=3.367\ LH^{1.5} \quad (1)$$

in which L=Weir Length (ft.), H=Head (ft.) and Q=Discharge (cfs). However, in metric units, the formula becomes:

$$Q=1.857\ LH^{1.5} \quad (2)$$

where L=Weir Length (m), H=Head (m) and Q=Discharge (m^3/s). The Cipoletti Weir used in the Laboratory was found to have Weir Length (L) = 0.142 m, hence the formula boiled down to:

$$Q= (0.263694\ H^{1.5}) \times 1000 \quad (3)$$

where H=Head (m) and Q=Discharge (L/s). This flow passing through the channel was controlled with the help of a flow regulating valve. The experimental setup has been shown with the help of a schematic diagram in Figure 2.

A Parshall flume of width 2.54 cm and a modified Parshall flume of width 3.18 cm were constructed and installed in the working section of the tilting channel. The dimensions of the Parshall flume and Modified Parshall flume used in the current study have been given in Table 1.

To ensure complete inflow of water through the Parshall flume and modified Parshall flume, wing walls were constructed and fitted at the entrance and exit of the flumes. A typical view of model Parshall flume has been shown in Figure 3.

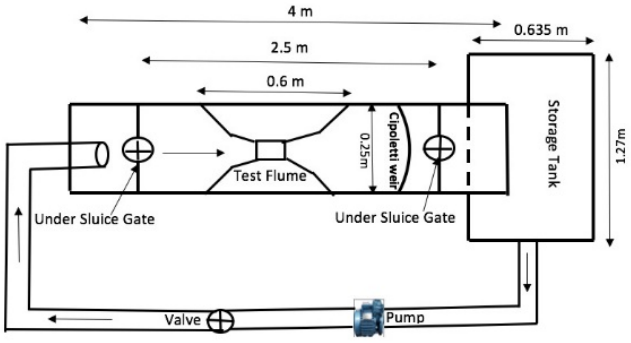

Fig. 2. Illustrative diagram of the experimental setup

Table 1.
Measurements of utilized models

S. No	Model	Width of the throat, W, cm	Length of the throat, F, cm	Height of Sill, K, cm
1.	Parshall flume	2.54	7.62	1.91
2.	Modified Parshall flume	3.18	8.57	1.98

Fig. 3. View of a Parshall flume model

To simulate longitudinal settlements, wooden planks were constructed and installed lifting the upstream section of the flumes, thereby creating a longitudinal differential settlement between the upstream and downstream sections of the flume. A series of 128 tests were conducted, with the flow rate ranging from 0.304 l/s to 4.936 l/s. Flume slopes of 0, 2.1, 4.2, and 6.3% were tested, with 32 tests being performed under each slope. During each test, the actual discharge, obtained using Cipoletti weir, and the measured discharge was recorded. The measured discharge was found using the relation given by [7];

$$Q=0.338\ H_a^{1.55} \quad (4)$$

where Q=Discharge (cfs) and H_a=Flow depth (ft). However, in Metric units the formula changes to:

$$Q=0.0479\ H_a^{1.55} \quad (5)$$

in which Q=Discharge (L/s) and H_a=Primary flow depth (cm).

The test procedure was same for all the 128 tests. Once the Parshall flume was installed at the target slope, flow was initiated. The flow took approximately 15 minutes after its initiation to achieve a steady-state. After achieving steady-state, the flow depth in the respective flume was measured at 2 specific points, namely H_a and H_b with the help of a point gauge. Utmost care has been taken while measuring H_a and H_b using point gauges with least count 0.01 mm. While H_a is the depth of water at a point $2/3^{rd}$ upstream of the crest of the flume, H_b is the depth just upstream of the junction of the throat and diverging section of the flume. Further, both the depths were measured taking the floor of the converging section as zero elevation. The locations of H_a and H_b have been shown in Figure 1. Consequently, the value of measured discharge was calculated corresponding to the actual discharge passing through the flume. After this, the discharge was increased, and the process was repeated. Upon successful completion of all tests for a particular slope, the slope was changed, and a similar test process was adopted for the new slope. Further, after completion of all the experiments for one flume, another flume was installed in the channel and the same process was repeated. With the actual discharge and measured discharge values for each of the 128 tests recorded, the Discharge Correction Factor (C_d) was computed as the ratio of actual discharge to the measured discharge which is given as:

$$C_d = \text{Actual discharge/Measured Discharge} \quad (6)$$

As mentioned earlier, since:

$$\text{Actual Discharge} = (0.263694\ H^{1.5}) \times 1000 \quad (7)$$

and

$$\text{Measured Discharge} = 0.0479\ H_a^{1.55} \quad (8)$$

Henceforth:

$$C_d = \{(0.263694\ H^{1.5}) \times 1000\} / (0.0479\ H_a^{1.55}) \quad (9)$$

So in this way, C_d for each of the 128 tests were computed. The dataset acquired by performing all the experiments has been presented in Table 2.

Table 2.
Experimental Dataset

Throat width of model, W, cm	Throat length of model, F, cm	Sill height of model, K, cm	Longitudinal slope, S, %	H_a, cm	H_b, cm	C_d, Output
2.54	7.62	1.91	0	4.66	2.96	0.584
2.54	7.62	1.91	0	8.92	7.92	0.821
2.54	7.62	1.91	0	12.1	8.64	0.892
2.54	7.62	1.91	0	14.65	10.03	0.88
2.54	7.62	1.91	0	17.3	12.33	0.879
2.54	7.62	1.91	0	19.49	14.55	0.84
2.54	7.62	1.91	0	20.95	15.64	0.845
2.54	7.62	1.91	0	21.83	16.23	0.866
2.54	7.62	1.91	0	5.2	0.73	0.493
2.54	7.62	1.91	0	8.7	3.42	0.853
2.54	7.62	1.91	0	12.14	7.06	0.889
2.54	7.62	1.91	0	14.89	9.71	0.858
2.54	7.62	1.91	0	17.55	12.43	0.86
2.54	7.62	1.91	0	19.51	14.02	0.84
2.54	7.62	1.91	0	21.03	15.54	0.841
2.54	7.62	1.91	0	21.86	16.17	0.864
2.54	7.62	1.91	2.1	3.62	0.83	0.864
2.54	7.62	1.91	2.1	8.28	2.46	0.921
2.54	7.62	1.91	2.1	11.58	5.27	0.955
2.54	7.62	1.91	2.1	14.22	7.66	0.922
2.54	7.62	1.91	2.1	16.67	11.31	0.931
2.54	7.62	1.91	2.1	18.74	12.87	0.894
2.54	7.62	1.91	2.1	20.22	13.79	0.893
2.54	7.62	1.91	2.1	21.18	15.24	0.907
2.54	7.62	1.91	2.1	4.77	1.44	0.563
2.54	7.62	1.91	2.1	8.6	2.52	0.869
2.54	7.62	1.91	2.1	11.48	5.86	0.968
2.54	7.62	1.91	2.1	14.13	8.35	0.931
2.54	7.62	1.91	2.1	16.76	11.55	0.923
2.54	7.62	1.91	2.1	18.66	12.91	0.899
2.54	7.62	1.91	2.1	20.11	14.26	0.901
2.54	7.62	1.91	2.1	21.16	15.2	0.908
2.54	7.62	1.91	4.2	4.6	0.5	0.596
2.54	7.62	1.91	4.2	8.09	2.31	0.955
2.54	7.62	1.91	4.2	11.7	6.37	0.94
2.54	7.62	1.91	4.2	14.03	7.86	0.941
2.54	7.62	1.91	4.2	16.79	10.67	0.921
2.54	7.62	1.91	4.2	18.58	12.52	0.906
2.54	7.62	1.91	4.2	20.01	14.48	0.908
2.54	7.62	1.91	4.2	20.96	14.79	0.922
2.54	7.62	1.91	4.2	3.66	2.13	0.85
2.54	7.62	1.91	4.2	7.83	2.2	1.005
2.54	7.62	1.91	4.2	11.57	5.89	0.956
2.54	7.62	1.91	4.2	14.15	8.16	0.929
2.54	7.62	1.91	4.2	16.59	10.58	0.938
2.54	7.62	1.91	4.2	18.75	12.5	0.893

Throat width of model, W, cm	Throat length of model, F, cm	Sill height of model, K, cm	Longitudinal slope, S, %	H_a, cm	H_b, cm	C_d, Output
2.54	7.62	1.91	4.2	19.95	13.89	0.912
2.54	7.62	1.91	4.2	21.05	14.5	0.916
2.54	7.62	1.91	6.3	5.15	1.2	0.5
2.54	7.62	1.91	6.3	9.07	3.66	0.8
2.54	7.62	1.91	6.3	11.9	5.48	0.916
2.54	7.62	1.91	6.3	13.68	8.34	0.979
2.54	7.62	1.91	6.3	17.07	10.52	0.897
2.54	7.62	1.91	6.3	19.17	12.8	0.863
2.54	7.62	1.91	6.3	20.63	14.18	0.866
2.54	7.62	1.91	6.3	21.57	15.8	0.882
2.54	7.62	1.91	6.3	5.31	0.75	0.477
2.54	7.62	1.91	6.3	7.34	1.39	1.111
2.54	7.62	1.91	6.3	12	5.9	0.904
2.54	7.62	1.91	6.3	14.57	8.42	0.888
2.54	7.62	1.91	6.3	17.2	10.85	0.887
2.54	7.62	1.91	6.3	19.32	12.91	0.852
2.54	7.62	1.91	6.3	20.66	14.38	0.864
2.54	7.62	1.91	6.3	21.57	14.83	0.882
3.18	8.57	1.98	0	5.03	1.48	0.516
3.18	8.57	1.98	0	8.03	2.28	0.966
3.18	8.57	1.98	0	10.69	4.49	1.081
3.18	8.57	1.98	0	13.15	6.61	1.041
3.18	8.57	1.98	0	15.28	8.76	1.066
3.18	8.57	1.98	0	16.89	10.45	1.05
3.18	8.57	1.98	0	18.15	11.74	1.056
3.18	8.57	1.98	0	19.11	12.5	1.064
3.18	8.57	1.98	0	4.3	1.79	0.662
3.18	8.57	1.98	0	8.03	2.03	0.966
3.18	8.57	1.98	0	10.6	4.44	1.096
3.18	8.57	1.98	0	12.81	6.3	1.084
3.18	8.57	1.98	0	15.47	9.07	1.045
3.18	8.57	1.98	0	17.04	10.59	1.037
3.18	8.57	1.98	0	18.23	11.52	1.049
3.18	8.57	1.98	0	19.08	12.47	1.067
3.18	8.57	1.98	2.1	4.88	1.14	0.544
3.18	8.57	1.98	2.1	7.72	1.59	1.027
3.18	8.57	1.98	2.1	10.62	4.09	1.092
3.18	8.57	1.98	2.1	12.89	6.25	1.073
3.18	8.57	1.98	2.1	15.27	8.38	1.066
3.18	8.57	1.98	2.1	17.13	10.19	1.027
3.18	8.57	1.98	2.1	18.57	11.63	1.019
3.18	8.57	1.98	2.1	19.44	12.43	1.036
3.18	8.57	1.98	2.1	4.47	1.02	0.623
3.18	8.57	1.98	2.1	7.84	1.42	1.003
3.18	8.57	1.98	2.1	10.67	3.94	1.084
3.18	8.57	1.98	2.1	12.99	6.38	1.061
3.18	8.57	1.98	2.1	15.34	8.44	1.059
3.18	8.57	1.98	2.1	17.34	10.17	1.008

Throat width of model, W, cm	Throat length of model, F, cm	Sill height of model, K, cm	Longitudinal slope, S, %	H_a, cm	H_b, cm	C_d, Output
3.18	8.57	1.98	2.1	18.5	11.53	1.025
3.18	8.57	1.98	2.1	19.29	12.47	1.049
3.18	8.57	1.98	4.2	4.77	0.13	0.563
3.18	8.57	1.98	4.2	7.93	1.52	0.985
3.18	8.57	1.98	4.2	10.65	3.81	1.088
3.18	8.57	1.98	4.2	13.04	5.95	1.054
3.18	8.57	1.98	4.2	15.48	8.33	1.044
3.18	8.57	1.98	4.2	17.35	9.89	1.007
3.18	8.57	1.98	4.2	18.72	11.26	1.007
3.18	8.57	1.98	4.2	19.5	12.04	1.031
3.18	8.57	1.98	4.2	4.39	1.2	0.641
3.18	8.57	1.98	4.2	7.52	0.87	1.07
3.18	8.57	1.98	4.2	10.7	3.64	1.08
3.18	8.57	1.98	4.2	12.89	5.87	1.073
3.18	8.57	1.98	4.2	15.23	7.93	1.071
3.18	8.57	1.98	4.2	17.13	9.86	1.027
3.18	8.57	1.98	4.2	18.37	11.1	1.037
3.18	8.57	1.98	4.2	19.25	11.84	1.052
3.18	8.57	1.98	6.3	5.05	0.65	0.516
3.18	8.57	1.98	6.3	7.84	1.1	1.003
3.18	8.57	1.98	6.3	10.59	4.07	1.097
3.18	8.57	1.98	6.3	13.16	5.51	1.039
3.18	8.57	1.98	6.3	15.56	7.67	1.036
3.18	8.57	1.98	6.3	17.46	9.32	0.997
3.18	8.57	1.98	6.3	18.46	11.29	1.029
3.18	8.57	1.98	6.3	18.74	11.41	1.097
3.18	8.57	1.98	6.3	3.73	0.22	0.825
3.18	8.57	1.98	6.3	7.16	0.45	1.154
3.18	8.57	1.98	6.3	9.99	2.91	1.201
3.18	8.57	1.98	6.3	12.41	4.78	1.139
3.18	8.57	1.98	6.3	14.89	7.77	1.11
3.18	8.57	1.98	6.3	16.87	8.81	1.052
3.18	8.57	1.98	6.3	18.11	10.64	1.06
3.18	8.57	1.98	6.3	19.01	11.61	1.073

2.2. Data set

The data set used in the soft computing techniques consisted of 128 experimental observations. Further, this data was bifurcated into 2 data sets, viz., Training dataset (88 observations) and Testing dataset (40 observations). Random selection was done from the total readings for the formation of the training dataset and testing dataset. The input parameters were Throat width of flume (W in cm), Throat length of flume (F in cm), Sill height of flume (K in cm), Longitudinal slope (S in %) and water depths at specific points (H_a in cm and H_b in cm) while the output parameter was Discharge correction factor (C_d). The salient features of training and testing datasets have been tabulated in Table 3.

2.3. Modelling techniques and application in the present problem

Multiple nonlinear regression (MNLR)

The usage of nonlinear regression is highly encouraged in cases where the linear models are not capable of modelling complex phenomena. In the present study, a multiple-nonlinear relationship has been considered by taking C_d as the dependent variable and the parameters W, F, K, S, H_a, and H_b as the independent variables. The nonlinear regression was established using training data set expressing C_d in terms of W, F, K, S, H_a, and H_b based on the following relationship:

$$C_d = (pr_1 \times W) + (pr_2 \times F) + (pr_3 \times K) + (pr_4 \times S) + (pr_5 \times H_a) + (pr_6 \times H_b) + pr_7 \quad (10)$$

where pr_1, pr_2, pr_3, pr_4, pr_5, pr_6, and pr_7 are constants associated with the corresponding variables. Application of Multiple nonlinear regression yielded the following relationship:

$$C_d = (0.0021 \times W) + (0.0791 \times F) + (-0.1085 \times K) + (-0.0047 \times S) + (0.0691 \times H_a) + (-0.0681 \times H_b) + 0.0942 \quad (11)$$

where W, F, K, H_a, and H_b are in cm and S is in %.

ANFIS

Adaptive Neuro-Fuzzy Inference System, also known as Adaptive Network-based fuzzy inference system (ANFIS), is a soft computing technique which integrates both fuzzy-logic and neural network principles, primarily because of its ability to encapsulate the benefits of both the techniques in a single structure [19]. Delving into the architecture of ANFIS reveals that the structure of ANFIS consists of five layers, namely the fuzzification layer, the rule layer, the normalization layer, the defuzzification layer, and the summation layer. Similar to ANN, ANFIS also uses a training dataset to realize its learning. In this way, the most suitable ANFIS structure about the target problem is obtained. This obtained structure is then subjected to a set of data points which the structure has never seen before, known as testing data. The aim of subjecting the obtained ANFIS structure to testing data is to see its impact on completely unknown data. The suitability of the subjected ANFIS structure is indicated by the error values given by the ANFIS model. Lower the error values, the more suitable the ANFIS model [20]. One such ANFIS based model developed using the Gaussian membership function (MF) has been shown in Figure 4.

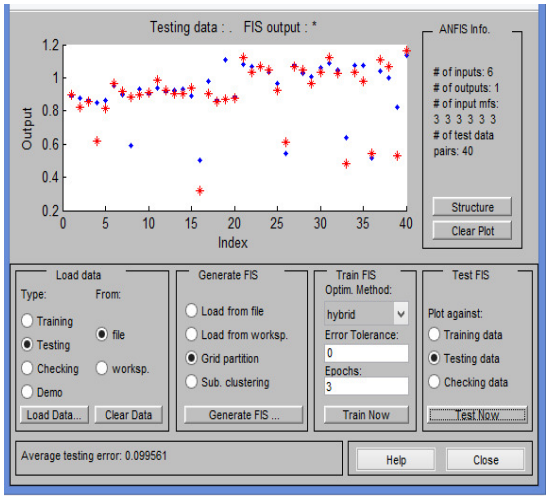

Fig.4. View of an ANFIS-based model

Table 3.
Features of Training Data and Testing Data

Training							
Parameter	W	F	K	S	H_a	H_b	C_d
Unit	cm	cm	cm	%	cm	cm	-
Min	2.54	7.62	1.91	0	3.62	0.13	0.477
Max	3.18	8.57	1.98	6.3	21.86	16.17	1.201
Mean	2.86	8.095	1.945	3.15	14.226	8.238	0.936
Median	2.86	8.095	1.945	3.15	15.37	8.94	0.948
Std. Deviation	0.321	0.477	0.035	2.361	5.468	4.860	0.148
Kurtosis	-2.047	-2.047	-2.047	-1.369	-1.102	-1.290	1.867
Skewness	-4.48227E-14	-8.3E-14	2.23E-13	6.48E-16	-0.441	-0.170	-1.309
Testing							
Parameter	W	F	K	S	H_a	H_b	C_d
Unit	cm	cm	cm	%	cm	cm	-
Min	2.54	7.62	1.91	0	3.73	0.22	0.5
Max	3.18	8.57	1.98	6.3	21.83	16.23	1.138
Mean	2.86	8.095	1.945	3.15	13.259	7.393	0.923
Median	2.86	8.095	1.945	3.15	13.905	8.245	0.935
Std. Deviation	0.324	0.481	0.035	2.377	5.104	4.525	0.163
Kurtosis	-2.108	-2.108	-2.108	-1.380	-0.868	-1.069	1.253
Skewness	-1.93997E-14	2.04E-14	6.9E-14	1.41E-15	-0.381	0.011	-1.290

Artificial Neural Network (ANN)

Artificial Neural Networks (ANNs) are computational programs biologically inspired by the neural networks constituting the animal brain. ANNs collect their knowledge by observing patterns in the input data and henceforth train themselves through experience, and not through programming.

A typical ANN consists of an input layer, one or more hidden layers, and an output layer. Each layer consists of Processing Elements (PEs), also known as artificial neurons inspired by the neurons present in the human brain. All the neurons are connected to each other. Technically, the connections are known as edges. Hence, neurons and edges together constitute a neural network. These neurons and edges have a coefficient associated with them, known as weight, which adjusts itself as the training proceeds [21].

After structuring of an ANN, it is required to train it. There are two ways to train a particular ANN, namely supervised learning and unsupervised learning [21]. In our current study, we have used a particular class of ANN of supervised learning where Multilayer Perceptron (MLP) has been utilized with the help of WEKA open-source software. In the case of MLP, the neurons do not form a cycle, and hence it is a type of feedforward neural network. Further, MLP uses a supervised learning technique known as backpropagation for its training. MLP is sometimes informally also referred to as a "vanilla" neural network, especially when it consists of only a single hidden layer [22]. Figure 5 shows an ANN structure developed for the current study consisting of 6 input variables constituting an input layer, 9 neurons constituting a hidden layer, and an output (C_d) constituting an output layer.

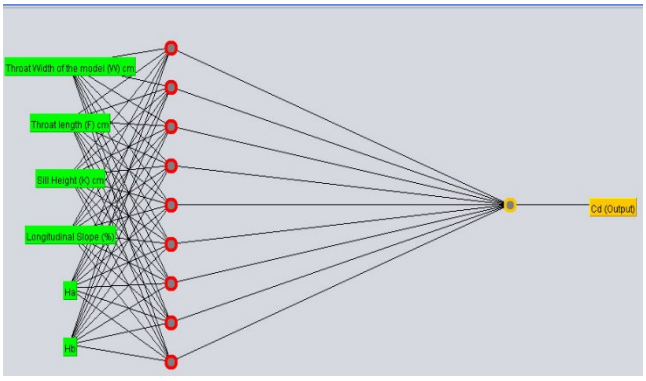

Fig. 5. View of an ANN structure

ANN has been used extensively for solving problems in the field of water resources engineering. I.A. Juma, et.al. [23] analysed hydraulic characteristics of hollow semi-circular weirs using ANN. Similarly, G. Tayfur, et.al. [24] applied MLP for estimating hydraulic conductivity in heterogeneous, unconfined aquifers. Furthermore, N.K. Tiwari, et.al. [25] applied ANFIS and ANN for the purpose of estimating the sediment removal efficiency of tunnel desilter. Lastly, N.K. Tiwari [26] implemented ANFIS, ANN and Fuzzy Logic (FL) with the aim of developing models which can be used for the estimation of oxygen aeration efficiency of hydraulic jump under sluice gate.

2.4. Implementation of ANFIS, ANN, and MNLR techniques

Implementation of ANN, ANFIS, and MNLR requires the optimization of user-defined parameters, which was performed by applying several trials on the training data set as well as the testing data set. The accuracy of each trial was evaluated using two widespread statistical measures, namely the Coefficient of Correlation (CC) and Root Mean Square Error (RMSE). The smaller value of RMSE concludes a closer estimation of the experimental data by models, whereas larger values of CC infers to a stronger matching of trends in the experimental data by the predictions of the model. The accepted values of various user-defined parameters obtained after several trials have been given in Table 4.

Table 4.
User-defined parameters for models

Technique	User Defined Parameters
ANFIS	No. of membership functions (MF_s): 3 3 3 3 3 3, Input MF Types: Gaussian MF(GAUSSMF), Triangular MF(TRIMF), Generalized Bell shaped MF (GBELLMF), Trapezoidal MF (TRAPMF)
ANN	Neurons:9, Learning Rate:0.3, Momentum:0.3, No. of Epochs: 500
MNLR	User defined Function:$Y=(pr_1\times X_1)+(pr_2\times X_2)+(pr_3\times X_3)+ +(pr_4\times X_4)+ (pr_5\times X_5)+(pr_6\times X_6)+pr_7$

3. Modeling results

3.1. Results of the MNLR model

The values predicted by the relationship obtained using the MNLR model were plotted against the observed values of their respective training as well as testing datasets, as shown in Figure 6.

Table 5.
Performance segment of the models

Model	Testing Data					Rank
	CC	RMSE	MAE	MSE	SDR	
ANFIS_GAUSSMF	0.8531	0.0998	0.0630	0.0099	0.0985	2
ANFIS_TRIMF	0.6937	0.2237	0.1250	0.0500	0.2255	4
ANFIS_GBELLMF	0.5100	0.7133	0.2590	0.5088	0.7090	5
ANFIS_TRAPMF	0.4818	0.6656	0.2330	0.4430	0.6605	6
ANN	0.8852	0.0776	0.0500	0.0060	0.0785	1
MNLR	0.7884	0.1023	0.0670	0.0104	0.1035	3

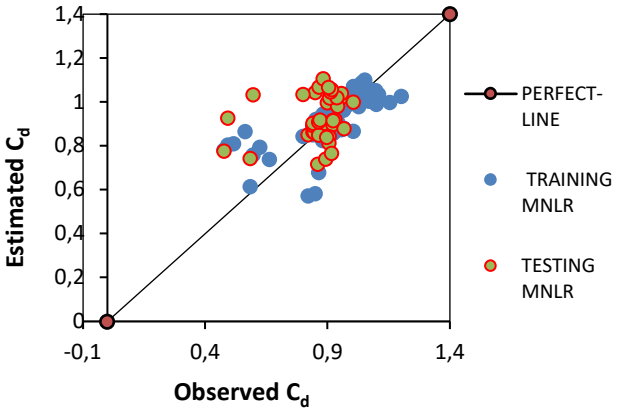

Fig. 6. Actual vs. Predicted Values of C_d using MNLR technique

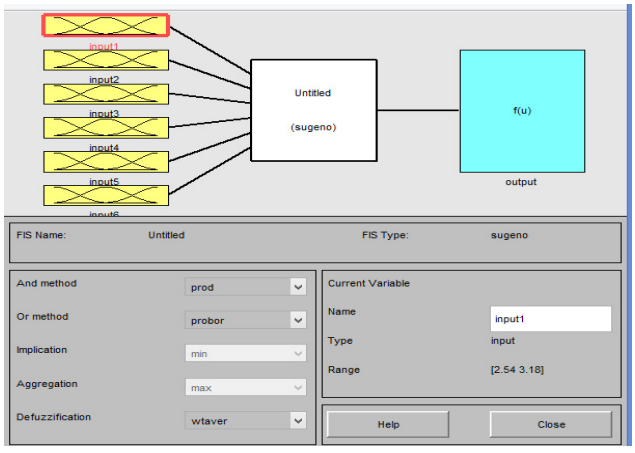

Fig. 7. Sugeno type of approach of ANFIS

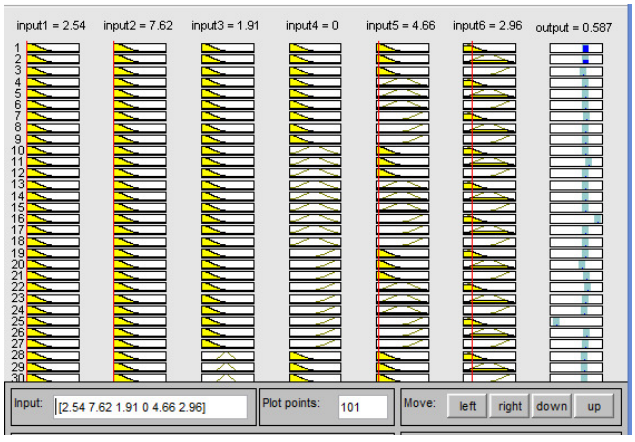

Fig. 8. Rules for C_d using Gaussian MF

The regression equation which has been plotted in the figure reveals that the predicted values of C_d of training and testing data points lie closer to the line of perfect agreement. This clearly indicates a good estimation by the developed functional relationship. The values of CC, RMSE, Mean absolute error (MAE), Mean Squared error (MSE) and Standard deviation for residual (SDR) yielded by testing data were 0.7884, 0.1023, 0.0670, 0.0104 and 0.1035 respectively (Tab. 5).

3.2. Results of ANFIS models

The development of ANFIS models was done using the hit-and trial process. Implementation of ANFIS in the current study was done using MATLAB, and it was a Sugeno type of approach, as shown in Figure 7.

Designing an ANFIS model involves defining the number of MF_s (membership functions) as well as input and output MF types. As an example, the rule diagram for C_d obtained using Gaussian MF (GAUSSMF) has been depicted in Figure 8. In the current study, five statistical measures, namely CC, RMSE, MAE, MSE and SDR yielded by different models obtained by adding different types of MF_s were evaluated one by one, and the performance of each of these models was examined by analysing the value of CC in case of testing data. As shown by Figure 9 and Table 5, the GAUSSMF based model exhibits the highest predictive accuracy with CC=0.8531. In fact, the values of other parameters, RMSE=0.0998, MAE=0.0630, MSE=0.0099 and SDR=0.0985 are also impressive. GAUSSMF is followed by TRIMF, GBELLMF, and lastly, TRAPMF based model.

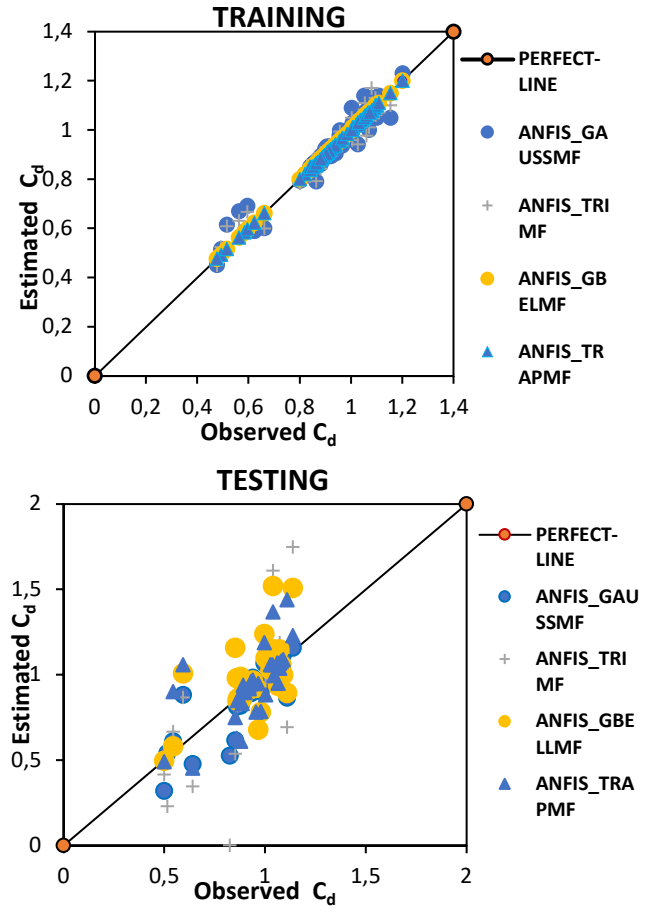

Fig. 9. Actual vs. Predicted Values of C_d using various ANFIS based model

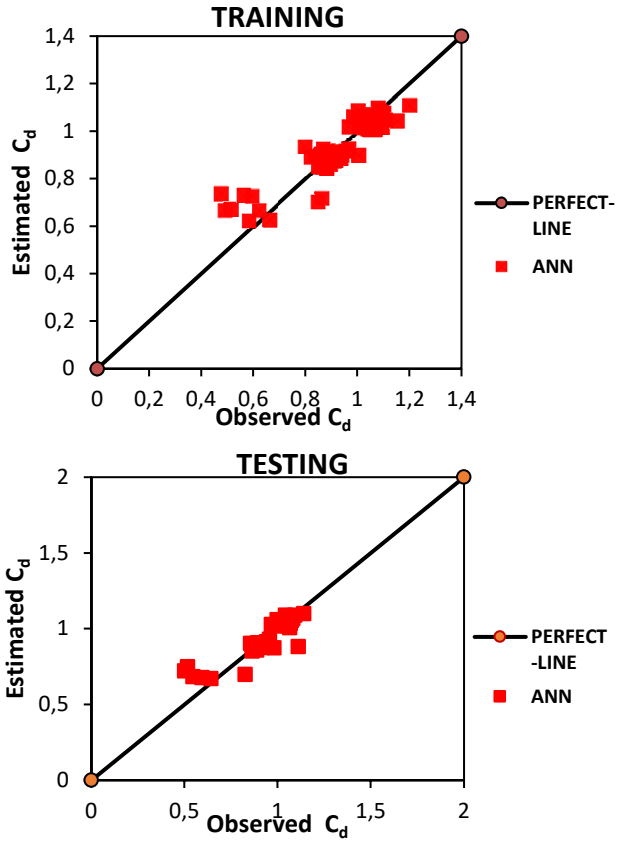

Fig. 10. Actual vs. Predicted Values of C_d using ANN

3.3. Results of the ANN model

The development of the ANN model was also a trial and error process. Multilayer Perception (MLP) was used for the purpose of modelling. After several runs, it was decided that the model used in the current study will consist of 1 hidden layer. The hidden layer consisted of 9 neurons, with Momentum=0.3, learning rate=0.3, and no. of epochs=500. The values of CC, RMSE, MAE, MSE and SDR obtained using this ANN model were 0.8852, 0.0776, 0.0500, 0.0060 and 0.0785 for the testing dataset. The performance of the ANN model has been shown in Figure 10.

3.4. Comparison of models

Comparison among ANFIS, ANN, and MNLR based models indicates that the ANN-based model showcases highest predictive accuracy as compared to other models as the value of CC is highest (Tab. 5) and values are lying very near to perfect line in comparison to other soft computing techniques, while the comparison within only ANFIS-based models shows that Gaussian MF-based model works better than other MF-based models.

To compare the performance of various models, the values of CC, RMSE, MAE, MSE and SDR yielded by each model on testing data were analysed, which has been summarised in Table 5. Using this methodology of performance evaluation, the overall ranking of various models in the prediction of C_d is as follows: ANN (1st), ANFIS_GAUSSMF (2nd), MNLR (3rd), ANFIS_TRIMF (4th), ANFIS_GBELLMF (5th) and lastly, ANFIS_TRAPMF (6th). The performance of various ANFIS based soft computing models has been shown in Figure 11.

3.5. Sensitivity analysis

To find out the most influential input variable in the prediction of C_d, a sensitivity analysis was conducted. Since the ANN-based model showed the highest predictive accuracy for the used data set, hence sensitivity analysis was also conducted using the ANN-based model only.

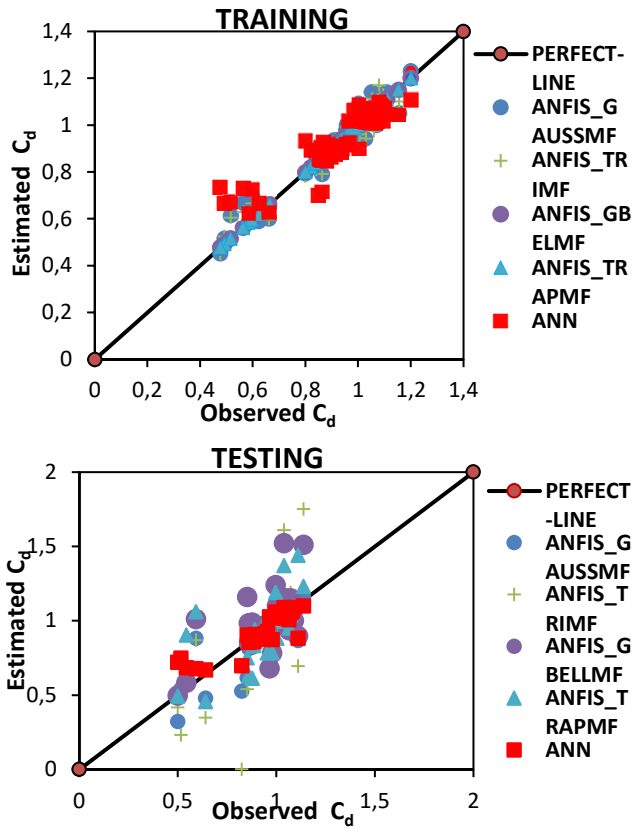

Fig. 11. Actual vs. Predicted Values of C_d using ANFIS and ANN approaches

Table 6.
Sensitivity analysis using the ANN-based model

Input combination	Input parameter removed	ANN	
		CC	RMSE
W,F,K,S,H_a,H_b	-	0.8852	0.0776
W,K,S,H_a,H_b	F	0.8238	0.0963
W,F,K,S,H_b	H_a	0.4693	0.149
W,F,K,S,H_a	H_b	0.7936	0.1017
W,F,S,H_a,H_b	K	0.8238	0.0963
W,F,K,H_a,H_b	S	0.8427	0.1008
F,K,S,H_a,H_b	W	0.8238	0.0963

Initially, sensitivity analysis was carried out by retaining all the input parameters simultaneously i.e. no parameter is removed and corresponding values of CC and RMSE were measured. Subsequently, different sets of training data were generated by pulling out one input variable each time, and the corresponding results were recorded for CC and RMSE yielded by the testing datasets. The results of this analysis have been summarised in Table 6. It can be deduced from the Table that H_a plays the most important role in the prediction of C_d as compared to other input parameters.

4. Conclusions

In this study, the experimental values of the discharge correction factor (C_d) observed for a standard Parshall flume of throat width 2.54 cm and a modified Parshall flume of throat width 3.18 cm were modelled. Using the MNLR technique, a relationship was established with C_d as a function of throat width of the flume, throat length of the flume, sill height of flume, longitudinal slope of flume, and flow depths H_a and H_b. Further, the performance of this relationship was compared with ANN and ANFIS based models. The ANN-based model was created using MLP, while 4-different shaped based ANFIS based models were created using a different membership function each time. The membership functions used were GAUSSMF, GBELLMF, TRIMF, and TRAPMF.

Based on the results obtained, it can be concluded that the ANN-based model with the highest value of CC and the lowest values of RMSE, MAE, MSE and SDR has highest predictive accuracy as compared to all other considered models. Amongst the ANFIS based models, GAUSSMF based model exhibits the highest predictive accuracy compared to GBELLMF, TRIMF, and TRAPMF based ANFIS models.

The predictive accuracy of the relationship established using the MNLR technique is greater than GBELLMF, TRIMF, and TRAPMF based ANFIS models, but inferior when compared to the ANN-based model and GAUSSMF based ANFIS model. Hence the relationship can be used in determining the values of C_d with reasonable accuracy with this data range. Further, sensitivity analysis suggested that H_a plays the most important role in the prediction of C_d in comparison to other input parameters.

References

[1] R.L. Parshall, Measuring water in irrigation channels with Parshall flumes and small weirs, United States Department of Agriculture, Circular 843 (1950) 1-62. Available from: https://mountainscholar.org/bitstream/handle/10217/185036/CERF_47-52_51_DIP.pdf?sequence=1&isAllowed=y

[2] R.L. Parshall, The Improved Venturi flume, Colorado Experiment Station, Colorado Agricultural College, Fort Collins Bulletin 336 (1928).

[3] D. Saran, N.K. Tiwari, S. Ranjan, Parshall Flumes: A Review, Proceedings of the Roorkee Water Conclave 2020, Roorkee, India, 2020, Paper no. RWC/56.
[4] V.M. Cone, The venturi flume, Journal of Agricultural Research 9/4 (1917) 115-123.
[5] F.A. Kilpatrick, V.R. Schneider, Use of flumes in measuring discharge, in: US Geological Survey Techniques of Water – Resources Investigations, 03-A14, US Geological Survey, 1983. DOI: https://doi.org/10.3133/twri03A14
[6] R.L. Parshall, Parshall flumes of large size, Colorado Agricultural and Mechanical College Extension Service Bulletin 426-A (1953).
[7] A.R. Robinson, Parshall measuring flumes of small sizes, Colorado Agricultural Experiment Station Technical Bulletin 61 (1957).
[8] S.R. Abt, K. Thompson, K. Staker, Discharge correction for longitudinal settlement of Parshall flumes, Transactions of the ASAE 32/5 (1989) 1541-1544, DOI: https://doi.org/10.13031/2013.31186
[9] S.R Abt, K.J. Staker, Rating correction for lateral settlement of Parshall flumes, Journal of Irrigation and Drainage Engineering 116/6 (1990) 797-803. DOI: https://doi.org/10.1061/(asce)0733-9437(1990)116:6(797)
[10] A.Genovez, S. Abt, B. Florentin, A. Garton, Correction for settlement of Parshall flume, Journal of Irrigation and Drainage Engineering 119/6 (1993) 1081-1091. DOI: https://doi.org/10.1061/(asce)0733-9437(1993)119:6(1081)
[11] S. Abt, A. Genovez, B. Florentin, Correction for settlement in submerged Parshall flumes, Journal of Irrigation and Drainage Engineering 120/3 (1994) 676-682. DOI: https://doi.org/10.1061/(asce)0733-9437(1994)120:3(676)
[12] S.R Abt, C.B Florentin, A. Genovez, B.C. Ruth, Settlement and submergence adjustments for Parshall flume, Journal of Irrigation and Drainage Engineering 121/5 (1995) 317-321. DOI: https://doi.org/10.1061/(asce)0733-9437(1995)121:5(317)
[13] B.J. Heiner, S.L. Barfuss, M.C. Johnson, Flow rate sensitivity due to Parshall flume staff gauge location and entrance wing wall configuration, Journal of Irrigation and Drainage Engineering 137/2 (2011) 94-101. DOI: https://doi.org/10.1061/(asce)ir.1943-4774.0000274
[14] B.M. Savage, B. Heiner, S.L. Barfuss, Parshall flume discharge correction coefficients through modelling, Proceedings of the Institution of Civil Engineers – Water Management 167/5 (2014) 279-287. DOI: https://doi.org/10.1680/wama.12.00112
[15] N.K Tiwari, P. Sihag, Prediction of oxygen transfer at modified Parshall flumes using regression models, ISH Journal of Hydraulic Engineering 26/2 (2020) 209-220. DOI: https://doi.org/10.1080/09715010.2018.1473058
[16] M. Kumar, N.K. Tiwari, S. Ranjan, Kernel function based regression approaches for estimating the oxygen transfer performance of plunging hollow jet aerator, Journal of Achievements in Materials and Manufacturing Engineering 95/2 (2019) 74-84. DOI: https://doi.org/10.5604/01.3001.0013.7917
[17] D. Bodana, N.K. Tiwari, S. Ranjan, U. Ghanekar, Estimation of the depth of penetration in a plunging hollow jet using artificial intelligence techniques, Archives of Materials Science and Engineering 103/2 (2020) 49-61. DOI: https://doi.org/10.5604/01.3001.0014.3354
[18] R.E Horton, Weir experiments, coefficients, and formulas, vol. 16, US Government Printing Office 1906. DOI: https://doi.org/10.3133/wsp150
[19] A. Abraham, Adaptation of fuzzy inference system using neural learning, in: N. Nedjah, L. Macedo Mourelle (eds), Fuzzy Systems Engineering. Studies in Fuzziness and Soft Computing, vol. 181, Springer, Berlin, Heidelberg, 2005, 53-83. DOI: https://doi.org/10.1007/11339366_3
[20] D. Karaboga, E. Kaya, Adaptive network based fuzzy inference system (ANFIS) training approaches: a comprehensive survey, Artificial Intelligence Review 52/4 (2019) 2263-2293. DOI: https://doi.org/10.1007/s10462-017-9610-2
[21] S. Agatonovic-Kustrin, R. Beresford, Basic concepts of artificial neural network (ANN) modeling and its application in pharmaceutical research, Journal of Pharmaceutical and Biomedical Analysis 22/5 (2000) 717-727. DOI: https://doi.org/10.1016/s0731-7085(99)00272-1
[22] T. Hastie, R. Tibshirani, J. Friedman, The elements of statistical learning: data mining, inference, and prediction, Springer, New York, 2009. DOI: https://doi.org/10.1007/978-0-387-84858-7
[23] I.A. Juma, H.H. Hussein, M.F. Al-Sarraj, Analysis of hydraulic characteristics for hollow semi-circular weirs using artificial neural networks, Flow Measurement and Instrumentation 38 (2014) 49-53. DOI: https://doi.org/10.1016/j.flowmeasinst.2014.05.003
[24] G. Tayfur, A.A. Nadiri, A.A. Moghaddam, Supervised intelligent committee machine method for hydraulic conductivity estimation, Water Resources Management 28/4 (2014) 1173-1184. DOI: https://doi.org/10.1007/s11269-014-0553-y

[25] N.K. Tiwari, P. Sihag, B.K. Singh, S. Ranjan, K.K. Singh, Estimation of Tunnel Desilter Sediment Removal Efficiency by ANFIS, Iranian Journal of Science and Technology, Transactions of Civil Engineering 44 (2020) 959-974.
DOI: https://doi.org/10.1007/s40996-019-00261-3

[26] N.K. Tiwari, Evaluating hydraulic jump oxygen aeration by experimental observations and data driven techniques, ISH Journal of Hydraulic Engineering (2019) 1-15.
DOI: https://doi.org/10.1080/09715010.2019.1658551